

DESIGN AND FABRICATION OF GRAVITY VORTEX TURBINE

Thesis submitted for the undergraduate degree in Mechanical Engineering
at the
University of Central Punjab



Project Members:

Muhammad Oraib Iqbal: L1F19BSME00014
Fahad: L1F19BSME00036
Daniyal Haider: L1F19BSME00018

Project Advisor:

Dr Gulraiz Ahmed

Session 2019-2023
Department of Mechanical Engineering,
University of Central Punjab, Lahore Pakistan

DESIGN AND FABRICATION OF GRAVITY VORTEX TURBINE

Thesis submitted for the undergraduate degree in Mechanical Engineering
at the
University of Central Punjab

Internal Examiner:

External Examiners:

Name and Title

Affiliation

Signature:

Name and Title

Affiliation

Signature:

Session 2019-2023
Faculty of Engineering,
University of Central Punjab, Lahore Pakistan

ABSTRACT

Gravitational water vortex turbine is a low head turbine which can operate on a head of about 1 to 1.5m with similar yield as conventional hydroelectric turbines characterized with positive environmental rejection. This study has been carried out in two phases. In the first phase, already present baffled type blades were used to obtain certain RPMs at the driver pulley. They were attached at different heights, but maximum RPMs were obtained at higher flowrate and at the bottom be designed and fabricated and the performance characteristics of the turbine will be compared in the second phase includes the design and fabrication of the conical basin with different cone angle by modifications in the same conical basin. Experimental tests will be carried out and the performance of the system with the use of a conical basin will be compared with that of the system using the conical basin with different cone angle and a turbine blade giving higher efficiency. A site testing will also be carried out to ensure the performance of the system.

DEDICATION

To Allah Almighty, my beloved parents, family and teachers, the reason for what I am today.

Thanks for your great support and continuous care.

ACKNOWLEDGEMENTS

In the name of Allah, the most beneficent and the most merciful, all praises Allah Almighty who showered his blessings upon us and gave us the will and strength to work on this project. May Allah always endow upon us his blessings in each and every field of life and make us a benefactor of human race. We would like to thank our Gracious Allah Almighty, who helped us to overcome all the obstacles that came on the way during the completion of our project. We received encouragement, support, and practical help from our teachers and university. It is pleasure to acknowledge their efforts and to show our gratitude.

We offer gratitude to Last Holy Prophet Muhammad (PBUH) who has given us the lesson of love, humanity, parity, justice, and also broken the cage of servitude for his golden sayings, ‘To seek knowledge is obligatory for every Muslim (male and female)’.

TABLE OF CONTENTS

ABSTRACT.....	I
DEDICATION.....	II
ACKNOWLEDGEMENTS.....	III
TABLE OF CONTENTS.....	IV
LIST OF FIGURES.....	VI
LIST OF TABLES.....	VII
LIST OF ABBREVIATIONS AND ACRONYMS.....	VIII
CHAPTER ONE: INTRODUCTION.....	1
1.1 Background.....	1
1.2 Working and Technicalities.....	2
1.3 CEP Attributes.....	3
1.4 Mapping with UN SDGs.....	3
CHAPTER TWO: LITERATURE REVIEW.....	4
2.1 Design of the runner.....	4
2.1.1 Assumptions.....	4
2.1.3 Vortex theory for runner design.....	4
2.2 Types of Basins.....	4
2.3 Types of Blades.....	6
2.4 Mechanism Used.....	7
CHAPTER THREE: DESIGN ANALYSIS AND FINDINGS.....	8
3.1 Experimental Analysis.....	8
3.1.1 Observations.....	8
3.1.2 Experimental Setup.....	9
3.1.3 Experimental Procedure.....	10
3.1.4 Tachometer.....	10
3.1.5 Measurements.....	11
3.1.6 Experimental Observation.....	12
3.1.7 Effect of Blade Position on RPMs using Baffled Blade.....	14
3.1.11 Proposed Blades.....	15
CHAPTER FOUR: FABRICATION.....	17
4.1 Blade Designing.....	17
4.1.1 CAD Drawing.....	17
4.1.2 Superimposition.....	18
4.1.3 Blade angle.....	18

4.1.4 Taper angle	18
4.1.5 Height ratio	19
4.1.6 Number of blade wings	19
4.1.7 3D Printed Model.....	20
4.1.8 Table calculations	20
4.1.9 Effect of Blade Position on RPMs using Conical Blade	21
4.2 Pulley Mechanism.....	22
4.2.1 Calculations	23
4.2.2 Varying smaller pulley diameter (d)	24
4.2.3 Varying Larger pulley diameter (D)	24
4.2.4 Varying center distance (S).....	25
4.2.5 Final selection	25
4.2.6 Power Transmission using optimum conditions.	26
CHAPTER FIVE: POWER CALCULATIONS.....	27
5.1 Theoretical Calculations	27
5.2 Experimental Calculations	28
5.3 Error Calculations	28
5.4 Generator Selection.....	28
CHAPTER SIX: CONCLUSIONS AND FUTURE DIRECTION	30
Appendix 1.....	31
Appendix 2.....	32
Appendix 3.....	33
References.....	35

LIST OF FIGURES

Figure 1.1 Forced Vortex [8]	1
Figure 1.2 Free Vortex	2
Figure 2.1 Flow simulation of cylindrical basin [11].....	5
Figure 2.2 Preliminary model of cylindrical basin [11].....	5
Figure 2.3 Flow simulation of conical basin [11]	6
Figure 2.4 Preliminary model with neck at the inlet of water collecting tub [5]	6
Figure 2.5 Types of blades [12]	7
Figure 2.6 Baffled type blade [12]	7
Figure 2.7 Pulley mechanism [6]	7
Figure 3.1 Rotor shaft	8
Figure 3.2 Outlet cross section of conical basin	9
Figure 3.3 Angle variation	9
Figure 3.4 GVT Model.....	10
Figure 3.5 Tachometer	11
Figure 3.6 Schematic Diagram.....	12
Figure 3.7 Experimental results of baffled blade (Appendix 1)	14
Figure 3.8 21 Blade Designs	15
Figure 3.9 Conical Blade	16
Figure 3.10 Turned Blade	16
Figure 4.1 Projection views of conical blade	18
Figure 4.2 Superimposed projection views of conical blade	18
Figure 4.3 Schematic Diagram (All dimensions are in centimeters)	19
Figure 4.4 3D Printed Model	20
Figure 4.5 Experimental results of conical blade (Appendix 2)	22
Figure 4.6 Pulley System Mechanism.....	23
Figure 4.7 Power Transmitted trend	26
Figure 5.1 DC Generator.....	Error! Bookmark not defined.

LIST OF TABLES

Table 1 CEP Attributes	3
Table 2 Measurements [fig.3.6]	11
Table 3 Comparison at different heights.....	13
Table 4 RPM VS Blade Position.....	21
Table 5 Varying smaller pulley diameter.....	24
Table 6 Varying larger pulley diameter	24
Table 7 Varying centre distance.....	25
Table 8 Varying center distance of smaller pulley	25
Table 9 Final selection	26

LIST OF ABBREVIATIONS AND ACRONYMS

CFD	Computational Fluid Dynamics
CEP	Complex Engineering Problem
d	smaller pulley diameter
D	Larger pulley diameter
DC	Direct Current
HR	Height Ratio
LED	Light Emitting Diode
N	No. of revolutions
PLA	Polylactic Acid
PET	Polyethylene terephthalate
PT_s	Power transmitted using optimum condition of smaller pulley variation.
PT_l	Power transmitted using optimum condition of larger pulley variation.
PT_{c2}	Power transmitted at a prime center distance using optimum condition of larger pulley.
PT_{c1}	Power transmitted at a prime center distance using optimum condition of smaller pulley.
PVC	Polyvinyl Chloride
RPMs	Revolutions Per Minutes
S	Center distance
UN SDGs	United Nations Sustainable Development Goals
WP	Work Package

CHAPTER ONE: INTRODUCTION

1.1 Background

This project is about design modification and practical testing of a Gravitation Vortex Turbine that is already fabricated by fall 15 batch students earlier in 2019. Gravitational Vortex Turbine can be used domestically at a very low head and has a good potential in providing electricity to remote communities. It is an economic and clean energy system that allows conversion of low head potential energy into kinetic energy to drive power turbine by using a gravitational vortex pool. The core objective of designing this turbine was to harness electrical energy from the river, canal, or tube well where water has the potential energy at a very low head which can be used to turn the blades of the turbine at certain revolutions per minute and generate power.

As we are familiar with the current energy crisis in Pakistan, it's need of the hour to design an alternative resource for electricity that can be used for domestic purposes. The core objective of designing this turbine is to harness electrical energy from the river or tube well where water has the potential energy at very low head which can be used to turn the blades of the turbine at certain revolutions per minute, before that water at certain velocity was passed from an inclined channel that has a neck at end which was connected to a water collecting tub in this way that a water vortex can be generated. The vortex turbine has curved blades installed at a certain height in the basin which will help to harness energy from the water vortex. After the blades attain certain revolutions per minute the shaft will help to transfer the motion to the driver pulley which will rotate the drive pulley ten times faster which has the direct current motor attracted to it on which we can run any twelve volts appliances. During design calculations it was found out that a plant having a water collecting tub with conical basin and curved vortex turbine blades was more efficient.

Vortex flow is defined as the flow of a fluid (water in our case) along a curved path. There are basically two types of vortexes. One is a free vortex, the other one is a forced vortex. When no external torque is required to rotate the fluid, that type of flow is called free vortex flow. Forced vortex is generated when an external force like a turbine is installed to rotate the water to create a vortex.



Figure 1.1 Forced Vortex [8]



Figure 1.2 Free Vortex

There are 2 gravitational vortex turbines installed already. One is in Indonesia and the other one is in France powering communities and villages with 50 to 500 households and generating 120.000 to 560.000 kWh per year per turbine [7]

Our experimental model is expected to extract a power of 1.5 to 3 W from a free vortex flow because our aim is to harness energy from the free vortex flow to rotate our turbine which then makes the generator move. Generator is a machine that produce electricity. Thus, electricity is produced via a free vortex flow.

This model needs a very low head i.e., 1 to 1.5 m. It is designed in such a way that maximum level of energy can be produced.

1.2 Working and Technicalities

Water at certain velocity is passed from an inclined channel that has a neck at end which is connected to a water collecting tub. In this way, a water vortex can be generated. The vortex turbine has baffled blades installed at a certain height in the basin which helps to harness energy from the water vortex. After the blades attain certain revolutions per minute, the shaft helps to transfer the motion to the driver pulley which then rotates the drive pulley ten times faster and has the direct current motor attracted to it on which we can run any 12 volts appliances.

Four different types of turbines were designed and analysed by our seniors and the performance characteristics were compared. Baffled turbine turned out to be the best option since it had more surface of contact with water and thus more rpms. Experimental tests were carried out and the performance of the system with the use of a conical basin was compared with that of the system using the cylindrical basin. Maximum vortex velocity for both cylindrical and conical basin is highest when the blade position is nearest to the outlet of the basin. The efficiency of a conical basin is higher than that of a cylindrical basin with the same number of turbine blades. Therefore, a plant having a water collecting tub with conical basin and baffled vortex turbine blades was more efficient [5]

We require a constant flow at the inlet of the turbine and the flowrate must be maintained i.e. inlet flowrate must be equal to the outlet flowrate. In order to ensure this effectively, we may install an inlet gate or a reservoir on the runner such that the flowrate of water remains constant.

1.3 CEP Attributes

These are all nine in numbers in which our project is mapping with 1st, 3rd, and 9th. First one indicates knowledge regarding vortex flow and its types, flowrate, and pulley mechanism. Whereas the third and ninth one indicates analysis and interdependence regarding the flowrate and velocity at different height and blade positions. Also, it indicates the analysis of different type of blades and basins.

Table 1 *CEP Attributes*

Attributes	Definitions
WP1	Depth of knowledge required
WP3	Depth of analysis required
WP9	Interdependence

1.4 Mapping with UN SDGs

These are 17 United Nations Sustainable Development Goals. Our project is mapping with 7th and 9th one. The seventh one is associated with ‘affordable and clean energy’ since we are not producing any sort of emissions in the environment, and it is easy and cheap to install as it doesn’t require any heads like in dams. The ninth one is associated with ‘industry, innovation, and infrastructure’ since it would be a major addition in the electricity production industries and it’s a totally new concept.

CHAPTER TWO: LITERATURE REVIEW

2.1 Design of the runner

The water vortex striking the turbine blades has been modelled as a jet of water striking the turbine blades like in crossflow or other impulse turbines. Taking the inlet jet angle to be 16° [10] and assuming no outlet whirl velocity, the design proceeds with the calculation of the inlet and outlet blade angles using velocity triangles.

2.1.1 Assumptions

Certain valid assumptions were made for the design of the model turbine which include neglecting head and pressure losses. The velocity at which the water strikes the runner is uniform along the length of the turbine. The flow in the water vortex is inviscid and irrotational because viscous effects are often negligible.

2.1.3 Vortex theory for runner design

Water vortex is generated when water swirls around an empty core of decreasing radius. A water vortex can be defined as a flow pattern with streamlines having concentric circles. Since all fluids have viscosity, no flow is truly irrotational, but flows can be successfully studied by assuming them to be inviscid and irrotational because of the negligible viscous effects [6]. In a free (irrotational) vortex, fluid particles do not rotate as they translate in circular paths around the vortex centre [6]. For an irrotational vortex, the radial velocity (V_r) is zero, while the tangential velocity (V_θ) is given by:

$$V_\theta = \frac{K}{2\pi r}$$

Where, K is the strength of the vortex and is defined as volume flow rate per unit depth [6].

$$K = \frac{Q}{h}$$

2.2 Types of Basins

Two types of basins can be used in gravitational vortex type turbine. One is the cylindrical basin and other one is the conical basin. Conical basin was proposed and CFD analysis was done through which it was concluded that free vortex stays for a longer time in a conical basin, and as a result stronger vortex is generated which produces more RPMs with the help of turbine blades mounted at the bottom of the vortex where vortex strength is highest as compared to the other heights, and it was found out during simulation on ANSYS Workbench, taking steady flow no slip condition to investigate the performance of different basin geometry on vortex velocity and its strength [5]

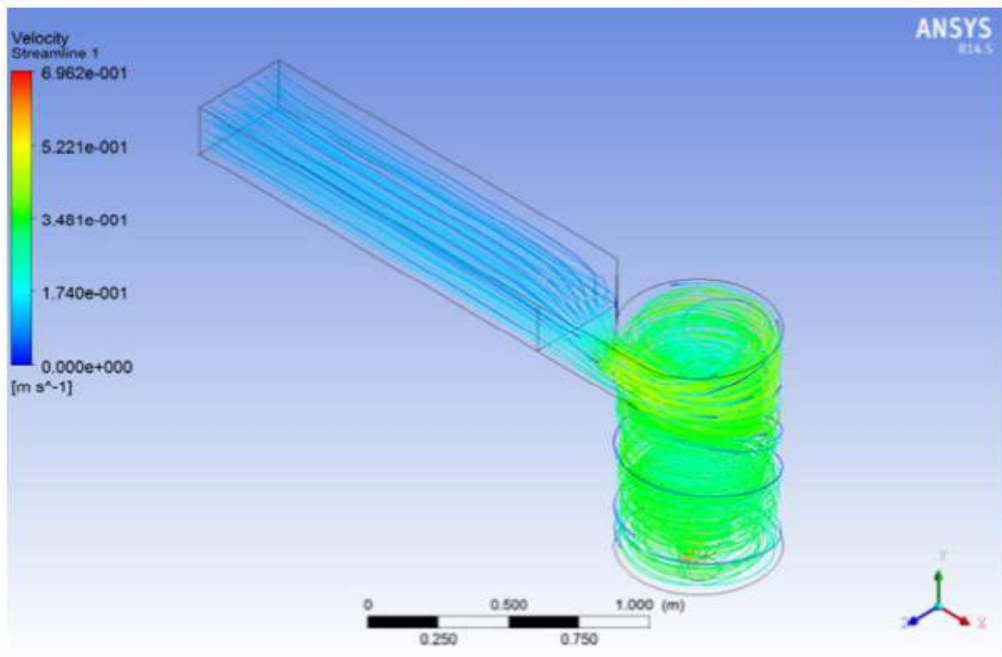


Figure 2.1 Flow simulation of cylindrical basin [11]

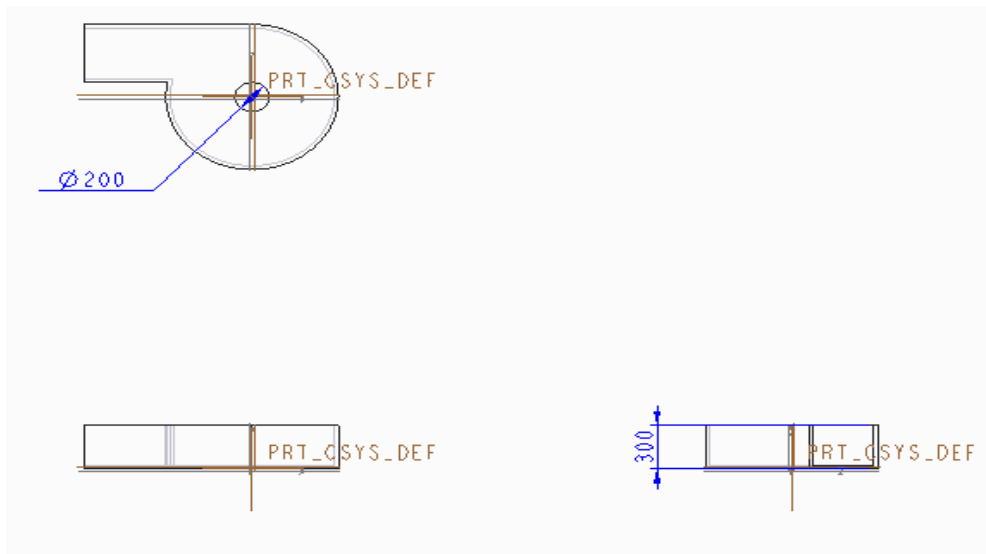


Figure 2.2 Preliminary model of cylindrical basin [11]

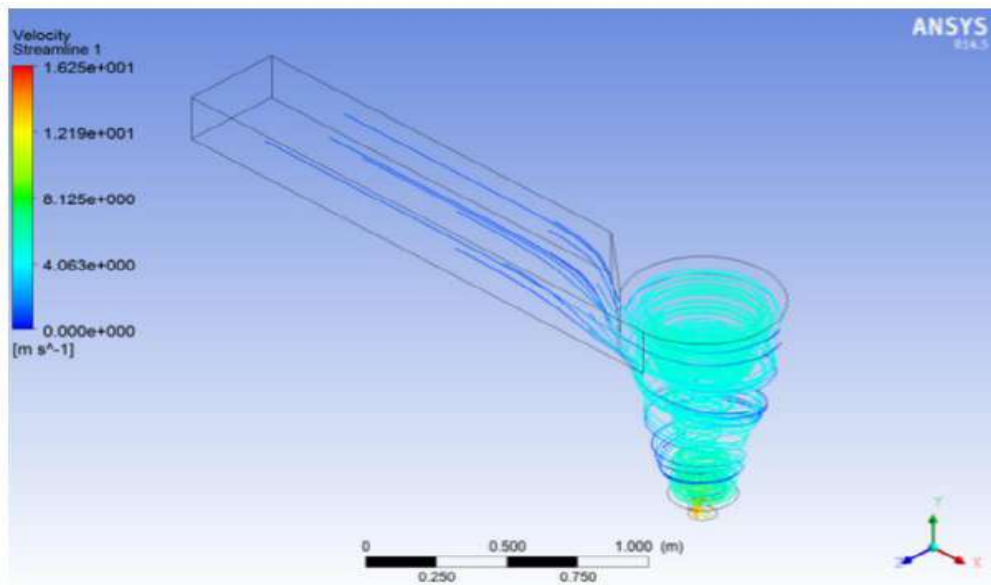


Figure 2.3 Flow simulation of conical basin [11]

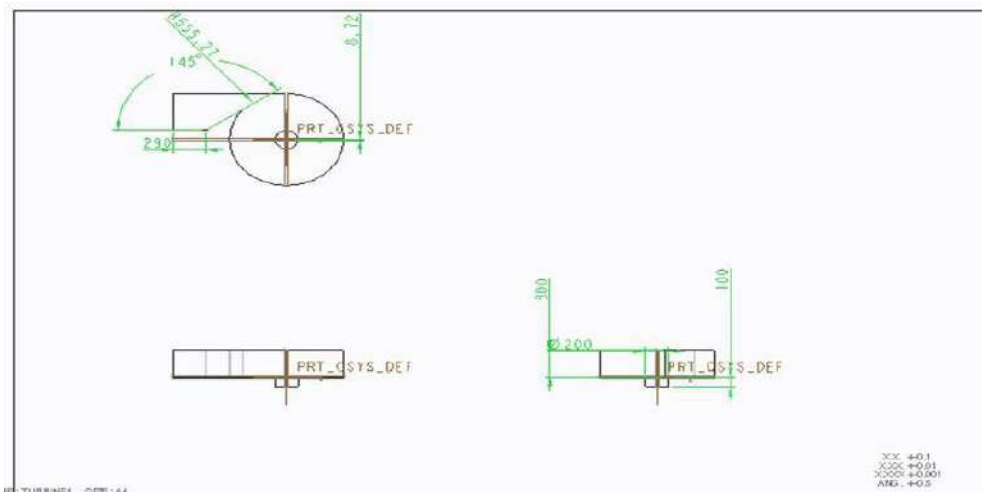
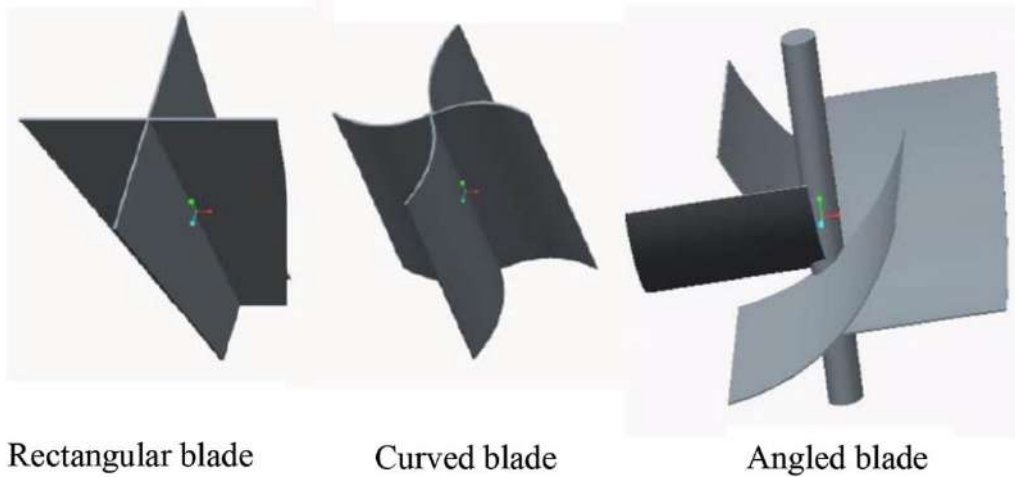


Figure 2.4 Preliminary model with neck at the inlet of water collecting tub [5]

2.3 Types of Blades

Four different types of blades were studied in the thesis namely rectangular, curved, angled, and baffled blades. After the research, baffled type blade was proposed which are basically curved blades but with the baffles at the top and bottom to capture more water. While experimental testing without installing pulley and dynamo motor, 132 RPMs [5] were recorded on a digital tachometer. Thus, it is concluded that the efficiency of the turbine depends on the design and number of blades, at a smaller number of blades greater efficiency is achieved as a greater number of blades cause distortion in the vortex. Moreover, if radii of the blade are increased, the efficiency decreases as the water velocity is low far away from the core [5]



Rectangular blade

Curved blade

Angled blade

Figure 2.5 Types of blades [12]

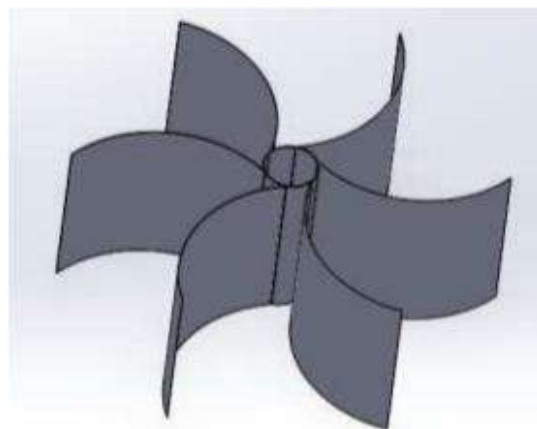


Figure 2.6 Baffled type blade [12]

2.4 Mechanism Used

The system involves the pulley and belt mechanism. In a belt and pulley system, a belt runs along a pulley's groove so that the power can be transferred either from one pulley to another or from the pulley directly to the application that requires power. Therefore, in our system we are interested in more RPMs and more power generation by installing a pulley and belt mechanism attached to a generator.

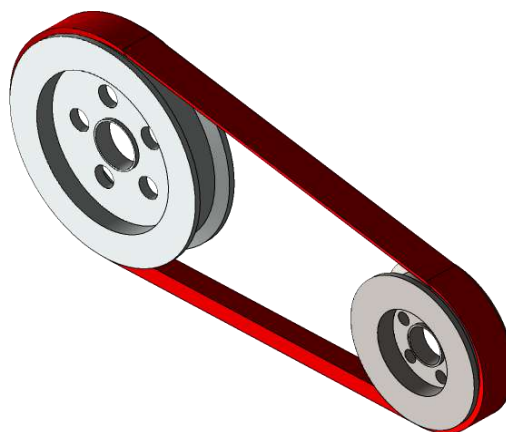


Figure 2.7 Pulley mechanism [6]

CHAPTER THREE: DESIGN ANALYSIS AND FINDINGS

The status of the project is deplorable. The overall apparatus is rusted, the bearings on the rotor shaft are destroyed, the housing of the bearings is quite heavy, the outlet cross sectional area of conical basin has some variations, the angle of the preliminary baffled type blade wings are deviated, the blade, rotor shaft, and pulley weight are too much, the inlet source pipes are not connected to the runner rather its manually supplied, the stepper motor is destroyed, the follower pulley is damaged, and there is no water recycling system and thus water is being wasted.

The project is brought into a working model and moving forward we have performed analysis on RPMs achieved on different blade positions at three different maintained head height (H). Listed below are the details of the analysis performed and our findings.

3.1 Experimental Analysis

The experimental analysis was performed without the pulley mechanism and the hurdles faced during the analysis and experimental procedures are described below.

3.1.1 Observations

Firstly, there was friction in the bearings because of which the rotation was rough and required constant force. It was impossible to get the blades rotated with those bearings. Therefore, we changed the bearings and installed NTN bearings of size 6006.



Figure 3.1 Rotor shaft

Next, we observed variations in cross sectional area of outlet which was creating disturbance in the outlet flowrate and was hindering our constant flowrate requirement.



Figure 3.2 Outlet cross section of conical basin

Then, we noticed that the blades were not at the same angle to each other and were deviated a little to their opposite side i.e., in clockwise direction.

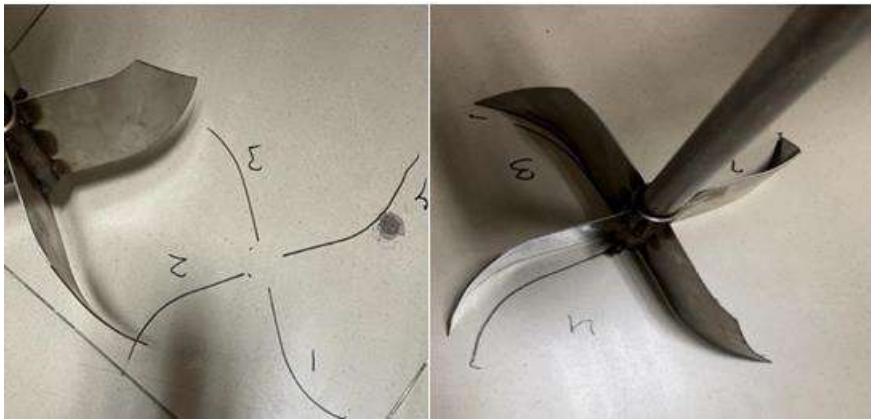


Figure 3.3 Angle variation

Next, we observed that the material of our shaft, blades, and pulley were not suitable. They were quite heavy considering the power we were planning to generate.

3.1.2 Experimental Setup

For performing the analysis, we have assembled our model in a way that we have removed the pulley mechanism and dynamo for now in order to perform all the testing. Our goal is to identify the best blade position at which the maximum RPMs are achieved and at what height it is possible.

We have installed a couple of ball bearings of size 6006 (30/55 mm) to ensure frictionless rotation of the shaft, PVC pipe (1.5 inches) at the outlet in order to decrease the flowrate, marked a scaler on our runner, shaft, conical basin in centimetres, installed (0.5 hp) pump so that to reuse the drained water, connected three pipes (two at the inlet and one for draining the tank into hydraulic bench), and fixed the outlet valve.

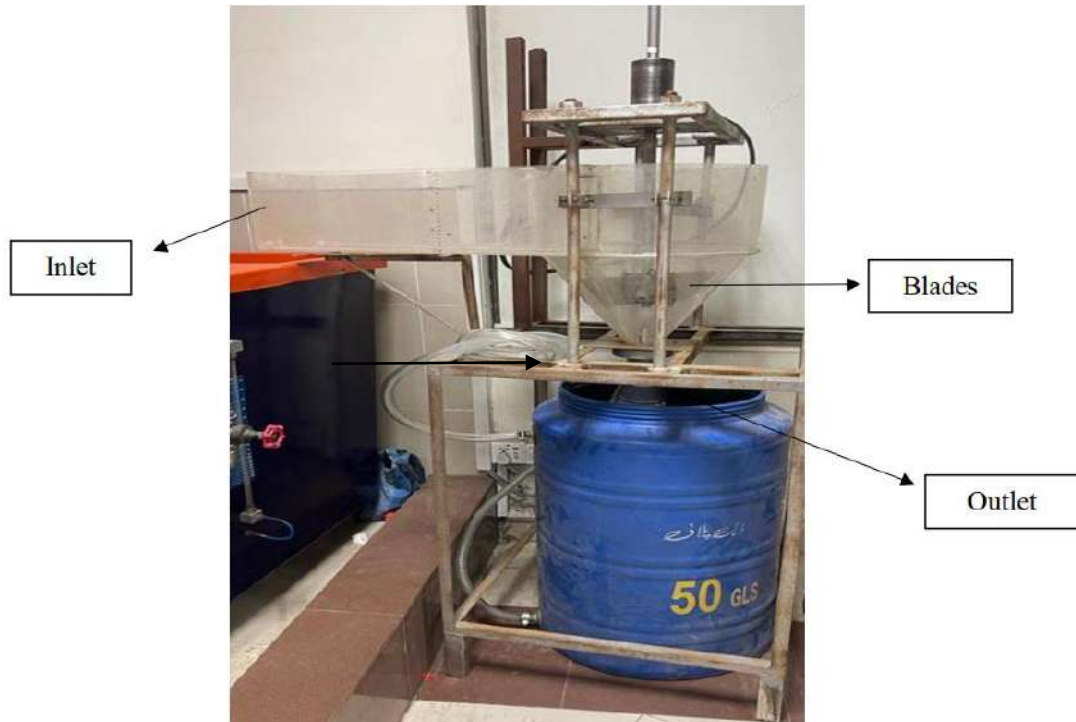


Figure 3.4 GVT Model

3.1.3 Experimental Procedure

Two pipes are placed at the inlet, first is coming from the main tank and the second is from the hydraulic bench. The water collected in our tank is pumped back into the hydraulic bench so that way we have negligible water wastage. First, we have pulled up the shaft combined with blades. Now, in order to have a constant velocity, we ensured that our inlet and outlet flowrates are equal by adjusting the flowrates of both the inlet and the outlet at a certain height i.e., at 35 cm. Once that is incorporated, we placed the shaft combined with blade back in our basin and tightened it on the lowest (reference) position and took the readings of rpm at that position from tachometer. Then, by increasing the blades height by 1cm each time (using the scale attached), we have identified the RPMs at different blade positions. Next, we have repeated the whole procedure for two more heights i.e., at 30 and 25 cm.

3.1.4 Tachometer

A tachometer works on the principle of relative motion. The device counts the number of rotations that the shaft makes per minute and displays it on the screen. First, we need to apply its magnet strip on the shaft and then by simply pointing the laser on that strip when the shaft is rotating, we'll have the rpms displayed.

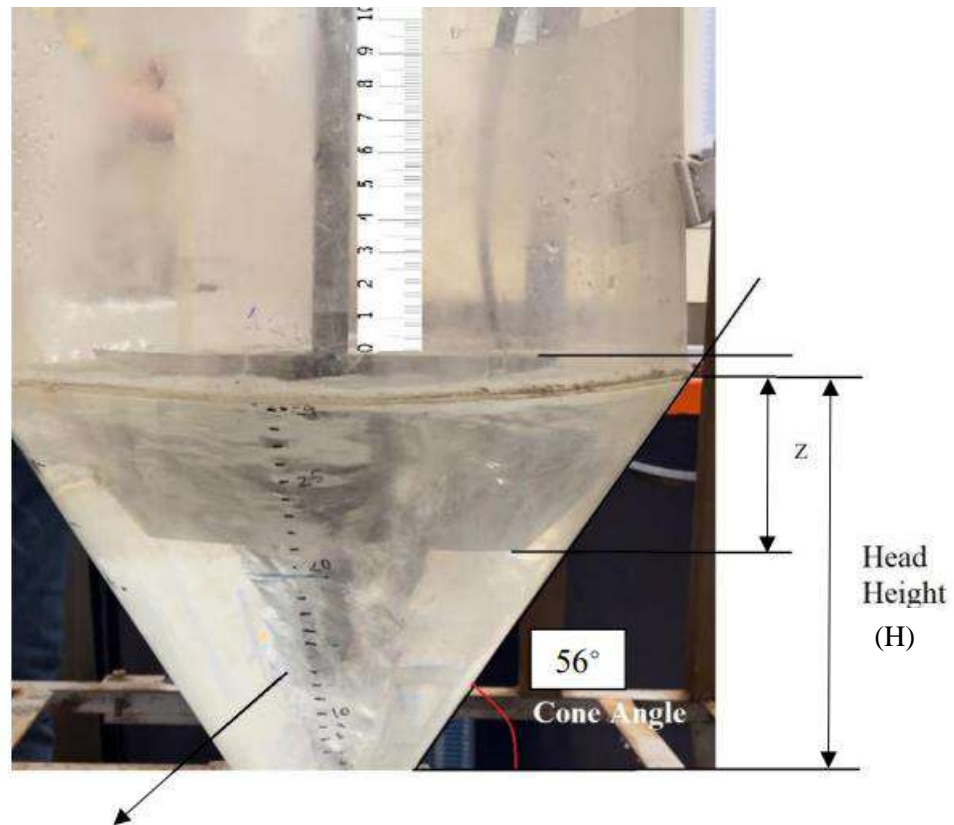


Figure 3.5 Tachometer

3.1.5 Measurements

Table 2 Measurements [fig.3.6]

Parameters	Measurements
Cone Height	25 cm
Cone Angle	56 degrees
Head Height (flowrate maintained)	35 cm
Head Height (flowrate maintained)	30 cm
Head Height (flowrate maintained)	25 cm
(Ref. point) z	9.2 cm



Vortex Flow

Figure 3.6 Schematic Diagram

3.1.6 Experimental Observation

We have calculated the inlet flowrate manually with the help of 2 litres measuring cylinder and a digital stopwatch. First, we turned on the valves and then to get rid of losses we waited half a minute until the flow became steady. Then, we filled the jug up to 2 litres and measured the time it took to reach that level. Finally, by using flowrate formula we calculated our flowrate in litres per second and then converted into cubic meter per second. Three observations and average of these were taken.

Since,
$$Q = V/t \quad (3.1)$$

(Flow rate of 1st pipe from main tank) $Q = 4.9 \times 10^{-4} \text{ m}^3/\text{s}$ using eq. (3.1)

(Flow rate of 2nd pipe from hydraulic bench) $Q = 5.1 \times 10^{-4} \text{ m}^3/\text{s}$ using eq. (3.1)

(Both together) $Q = 8.6 \times 10^{-4} \text{ m}^3/\text{s}$ using eq. (3.1)

Pipe from pump was discharged in the hydraulic bench so that we have zero water wastage during our testing phase. Three trials were taken and the average flow rate from pump was found.

(Average flowrate of pump) $Q = 2.36 \times 10^{-4} \text{ m}^3/\text{s}$ sing eq. (3.1)

Similarly, we calculated the outlet flowrate manually with the help of a conical basin and a digital stopwatch. First, we closed the basin (outlet) valve and filled it up to 12 liters (priorly marked the point) and then after some time we opened the basin (outlet) valve and measured the time it took to drain. Finally, by using flowrate formula we calculated our flowrate in liters per second and then converted it into cubic meters per second. Note that we performed three trials and then found out the average flowrate.

(Average outlet flowrate)
$$Q = 1.93 \times 10^{-4} \text{ m}^3/\text{s} \quad \text{using eq. (3.1)}$$

The diameter of the outlet cross section of the conical basin was 1.5 cm which is 0.0381 m.

Then, we calculated the average velocity by taking three trials.

Since,
$$v_{avg} = \frac{4Q}{\pi D^2} \quad (3.2)$$

(Average outlet velocity)
$$v_{avg} = 1.67 \text{ m/s} \quad \text{using eq. (3.2)}$$

Table 3 Comparison at different heights

Height maintained at 35 cm		Height maintained at 30 cm		Height maintained at 25 cm	
$Q = 9 \times 10^{-4} \text{ m}^3/\text{s}$		$Q = 8 \times 10^{-4} \text{ m}^3/\text{s}$		$Q = 6 \times 10^{-4} \text{ m}^3/\text{s}$	
Blade Position	RPM	Blade Position	RPM	Blade Position	RPM
0	128	0	103.5	0	87
1	122	1	102	1	82
2	116	2	90.5	2	75
3	112	3	92	3	71.5
4	114	4	83	4	69
5	102	5	84.5	5	62
6	92	6	71.5	6	55
7	96	7	74.5	7	40
8	88	8	67.5	8	30
9	83	9	64	9	21
10	78	10	52.5	10	14

3.1.7 Effect of Blade Position on RPMs using Baffled Blade

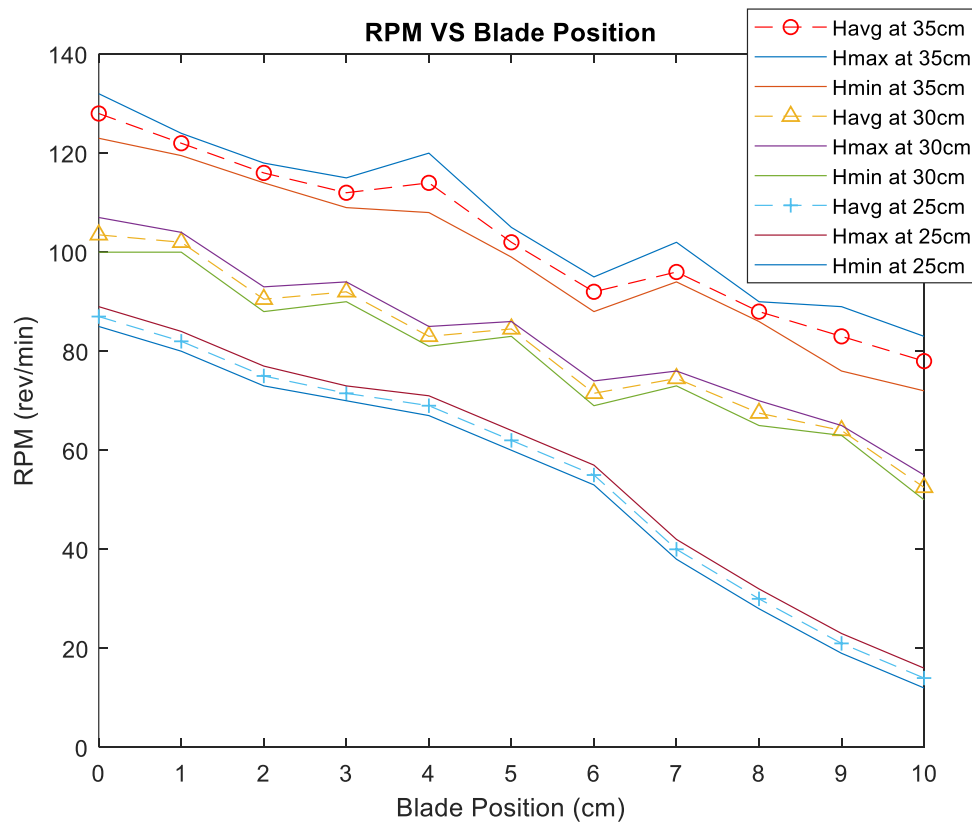


Figure 3.7 Experimental results of baffled blade (Appendix 1).

We analysed the RPMs received at three different maintained heights i.e., at 35 cm, 30 cm, and 25 cm. The graph shows a decreasing trend towards rpm as we move upward by increasing the blade position by 1 cm each time for all three of the maintained heights. That is, at 35 cm, 30 cm, and 25 cm it gives higher RPM values when the blade is in lowest (reference) position. Moving forward as the blade position is increased, the RPMs decrease gradually. At 35 cm, we received a range of (128 to 78) RPMs at (0 to 10) cm blade positions. At 30 cm, we received a range of (103.5 to 52.5) RPMs at (0 to 10) cm blade positions. At 25 cm, we received a range of (87 to 14) RPMs at (0 to 10) cm blade positions. Thus, we can conclude that by decreasing the maintained height, our RPMs decrease as well and vice versa. We noticed 15.9% increase in RPM generation by increasing the head height maintained from 25 cm to 30 cm. However, when we moved from 30 cm to 35 cm we observed a percentage increase of 19%.

Henceforth, we gathered some key takeaways which are described further. The more the height of the flowrate is maintained i.e., 35 cm and greater, the more are the RPMs received i.e., 130 and greater. The blade at the lowest (reference) position gives the maximum RPM value since the vortex strength is highest at the bottom and it gets lower moving up. Lower the weight of the blades, the shaft, and the pulley, higher will be the RPMs received. Considering that, we have specified our selection below in the next paragraph. Bearings used should be totally frictionless and of the lowest value of friction i.e., NTN bearing (6006).

3.1.11 Proposed Blades

We consulted various research papers studying designs of blades and conclusions drawn from each of them. The design ultimately depends upon the experimental setup in which some were based on cylindrical basin and some of them were for conical basin. Our system contains a conical basin, so the research paper with 21 blade designs turned out to be more relevant for us. A thorough analysis has been performed using these 21 blades and the operating speed of the runner turned out to be 50–80 RPM, and hence, the study of torque was carried out in this speed range [3]

The several parameters used in the design of the blade are blade angles in vertical plane and horizontal plane, taper angle, height ratio, and the number of blade wings. For each of the parameters varied, the power and torque variation would be small. The bigger picture is only visible when the range of power and torque variations are determined since each of the parameters has a small contribution to increasing the turbine power production [3]. The height ratio is the parameter to be most cared for since this affects the power generation largely [3]. The efficiency of the Gravitational Vortex Turbine (GVT) can be improved by the selection of optimum geometrical parameters [3]



Figure 3.8 21 Blade Designs

According to our experimental setup and literature research, conical [fig. 3.9] and turned blades [fig. 3.10] would be more appropriate and suitable. Since, our system contains a conical basin, we would be designing the taper angle of the blade conforming the cone angle

of the basin ensuring to reduce water seepage from the sides of the turbine. Moreover, we are drafting a blade having 3 sections all together so that we do not need to fabricate 3 blades separately and our analysis could be carried out more conveniently.

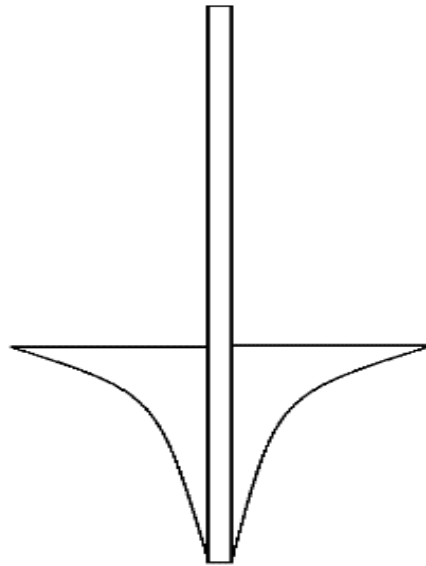


Figure 3.9 Conical Blade



Figure 3.10 Turned Blade

CHAPTER FOUR: FABRICATION

4.1 Blade Designing

We selected the conical turbine since they were found to be the best option through our research and calculations. This turbine has a tapered profile from the root to the tip. The tapered geometry distributes the stress more evenly along the blade, making it more resistant to bending and torsion forces that occur during operation. The conical shape provides inherent structural strength to the blade. As our fluid flows through the runner into the basin (cone), the tangential velocity generated is converted into z-axis along the way down into the sink. We are utilizing that and have considered it while designing our blade geometry since according to our findings, the maximum strength is achieved there. Moreover, we are assured that the frequency at which the incoming fluid strikes the blade increases by increasing the surface area. While designing the blade, the height ratio is the most influential parameter since the blade surface area changes rapidly with a change in height. The power coefficient tends to decrease at a higher height ratio since water drag and turbine weight start dominating the power production capacity of the turbine. Our turbine consists of four wings. All the four wings are evenly spaced around the circumference of the blade and extend from the root to the tip. These wings are designed to efficiently capture the energy of the fluid flowing over them and convert it into rotational motion. We selected a polylactic acid (PLA) material and 3D printed our model [fig. 4.4] after prepping its assembly on Creo Parametric [fig. 4.1]. Some factors like height ratio, taper angle, blade angle, and the number of wings of blade were worked upon while designing the blade which are discussed later in this section.

4.1.1 CAD Drawing

Observing our research, analysis, and calculations we have prepared an assembly of our selected turbine using Creo Parametric. We have splitted our model into 3 sections so that to be able to perform our analysis on each of them separately and together as well in order to achieve maximum power extraction from the vortex and ultimately maximum efficiency from our working model.

First blade section height is i.e., 9.3 cm [fig. 4.3] which is slightly larger than our previous baffled type blade all because to utilise maximum energy from our vortex flow. The second blade section height is 3.8 cm [fig. 4.3] and the third blade section height is 3.1 cm [fig. 4.3]. The tangential velocity being created as soon as the water leaves the runner is converted into z-axis, so by increasing the height of the 1st blade and connecting 2nd, and 3rd blade sections as well during our analysis are all our strategic techniques to get maximum energy from our vortex.

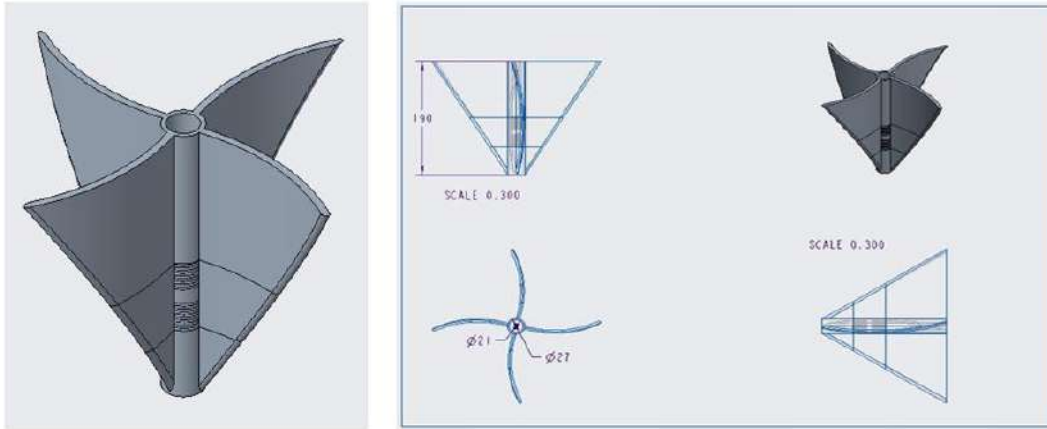


Figure 4.1 Projection views of conical blade

4.1.2 Superimposition

Superimposition is the placement of a model on top of an already-existing model to conceal something. In our case, we have superimposed our already existing baffled blade over our selected conical blade [fig. 4.2] and analyzed our findings practically by considering the parameters like; blade angles, taper angle conforming the basin cone, height ratio, and number of blade wings.

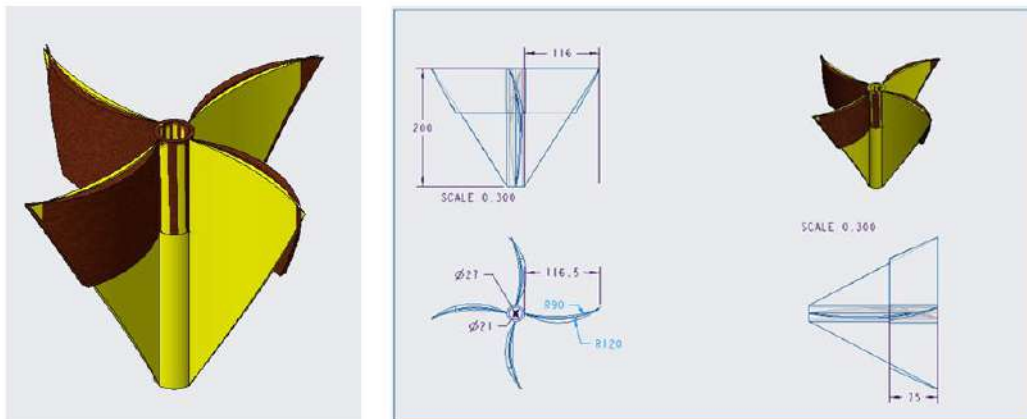


Figure 4.2 Superimposed projection views of conical blade

4.1.3 Blade angle

The blade angle is limited to R150 because the blades angle in vertical plane eventually disturbs the vortex formation and thus decreases the power coefficient with an increase in the blade angle. However, the blade angle introduced in horizontal plane does not disturb vortex formation.

4.1.4 Taper angle

We have opted for 34 degrees taper angle conforming the cone angle (56 degrees) of the basin. Seepage plays a huge role here, and we have ensured that by using this condition our

water seepage decreases from the sides of the turbine to a certain limit so that to maintain the circulation of water around the basin.

4.1.5 Height ratio

The height ratio is the most influential parameter since the blade surface area changes rapidly with a change in height. The power coefficient tends to decrease at a higher height ratio since water drag and turbine weight start dominating the power production capacity of the turbine.

$$\text{Height ratio (HR)} = \frac{\text{Turbine height}}{\text{Basin height}}$$

Therefore, we have calculated the height ratios using all 3 blade sections together, 2 upper blade sections together, 2 lower blade sections together, and 1 upper blade section. Height ratio of 3 blade sections together was 0.64, 2 upper blade sections together had a height ratio of 0.51, 2 lower blade sections together had a height ratio of 0.28, and finally 1 upper blade section only had a height ratio of 0.38.

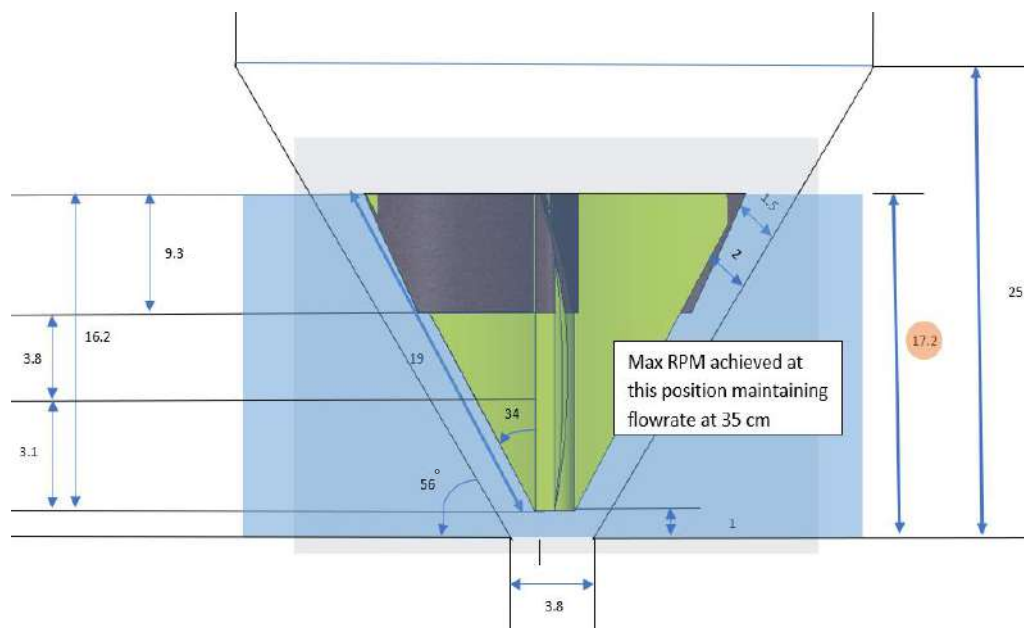


Figure 4.3 Schematic Diagram (All dimensions are in centimeters)

The maximum rpm achieved was at the reference point which is 1 cm above the sink using all 3 parts of the turbine.

4.1.6 Number of blade wings

The turbine with 4 blade wings has the highest power coefficient. The increment of the blade number makes the turbine capable of handling a large amount of flow efficiently. The frequency at which the incoming fluid strikes the turbine increases. The negative effect of using more blades in a single turbine is that the weight of the turbine increases along with drag loss.

4.1.7 3D Printed Model

We selected a polylactic acid (PLA) material and 3D printed our model [fig. 4.4] after prepping its assembly on Creo Parametric [fig. 4.1]. The total weight of the final model was estimated to be 230 grams with an infill density of 80%

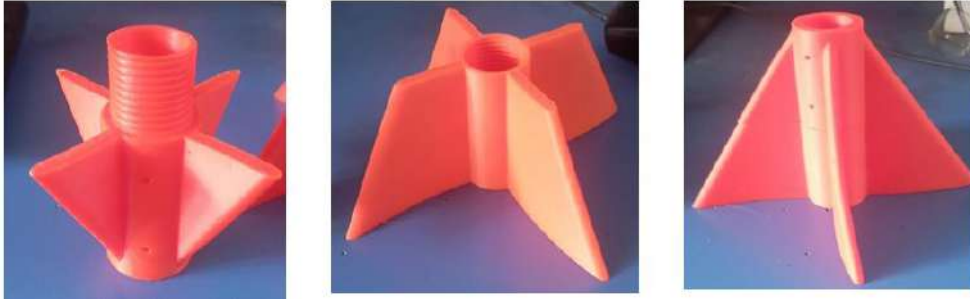


Figure 4.4 3D Printed Model

4.1.8 Table calculations

First, by using the upper section of the blade alone, we found our reference point to be at 6.9 cm and by displacing it upward from this point we performed our experimental analysis as shown in the table.

Second, by using the upper and middle blade sections together, we found our reference point to be at 3.1 cm and by displacing them upward from this point we performed our experimental analysis as shown in the table.

At last, by using all the three blade sections together, we found our reference point to be at 1 cm and by displacing it upward from this point we performed our experimental analysis as shown in the table.

Table 4 RPM VS Blade Position

Height maintained = 35 cm			
Blade Position (cm)	RPM (using upper part)	RPM (using upper and middle part)	RPM (using all three parts together)
0	129	111	145
1	121.3	114	131
2	116.5	110	126
3	110	105	121
4	109	99	128
5	106.5	102	118
6	100.6	97	119
7	94.3	92	109
8	88	84	123
9	92	88	112
10	88.3	81	108
11	84	0	99
12	0	0	75
13	0	0	83
14	0	0	71
15	0	0	74

c

4.1.9 Effect of Blade Position on RPMs using Conical Blade

We have plotted a graph between RPM and blade position. The highest position of our turbine is considered as a reference point and from this reference position we have moved 15 cm above. Our blade is divided into three parts. First, we used the upper part of the blade for our analysis. The maximum RPMs we achieved using a single blade was 129 RPMs. It was obtained at the reference point. Then we joined the middle part with the upper part and carried out our analysis. The maximum RPMs we achieved was 111 RPMs and these were at the reference point. Finally, we joined all the three parts and carried out our analysis and the maximum RPMs achieved were 145 RPMs. Thus, we can conclude that the maximum RPMs can be obtained as we move close to the cone because the strength of the vortex is more at the lowest part of the cone.

We noticed 13.9 % increase as we shifted from 1 blade section to 2 blade section. Moving forward, as we shifted from 2 blade section to 3 blade section, we noticed a percentage increase of 11 % in RPM generation.

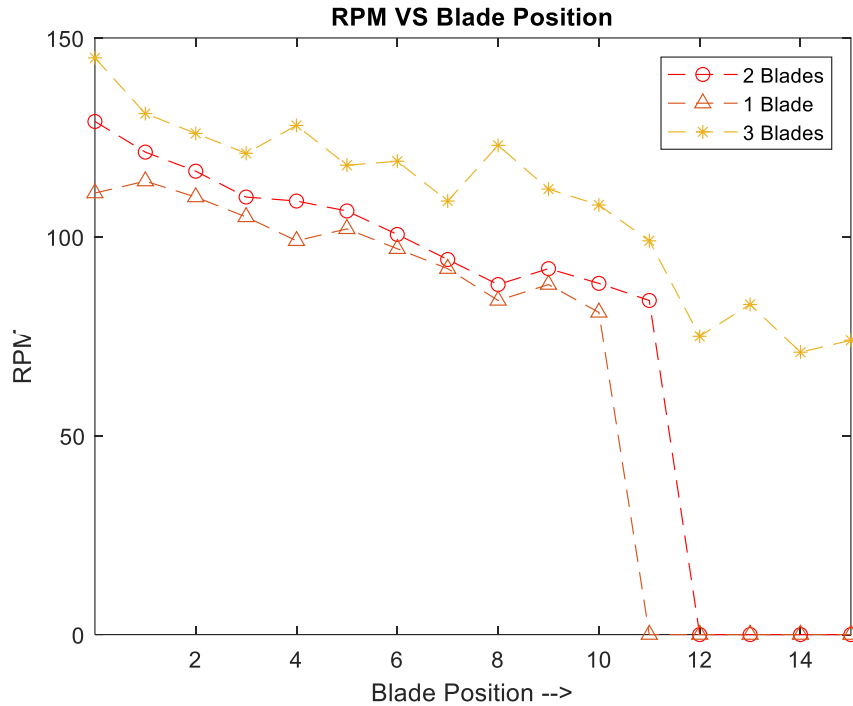


Figure 4.5 Experimental results of conical blade. (Appendix 2)

4.2 Pulley Mechanism

For our model we have installed a single belt and pulley mechanism to increase the RPMs and our overall power production. The belt and pulley system are a method of transferring power from one rotating shaft to another. It is a simple and effective system that uses a belt to connect pulleys on the two shafts. The material we used was polyethylene terephthalate (PET) since it's strong, lightweight and 100% recyclable characteristics turned out to be ideal in our case. The belt wraps around the pulleys and uses friction to transfer power from one shaft to the other.

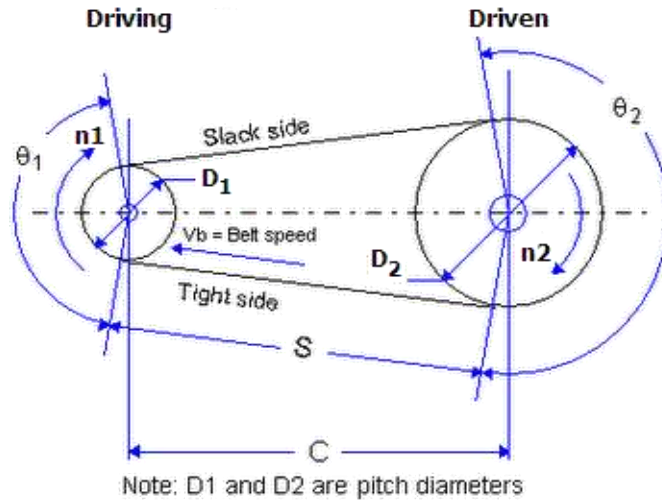


Figure 4.6 Pulley System Mechanism

Where, D_1 is diameter of the smaller pulley, D_2 is diameter of the larger pulley, C is span, S is center distance, θ_1 is angle of contact, θ_2 is angle of lap, ω_1 is revolutions on smaller pulley, and ω_2 is revolutions on larger pulley.

4.2.1 Calculations

The center distance between pulleys (S) is 31 cm, the radius of larger pulley (R) is 13 cm, the radius of smaller pulley (r) is 5 cm.

$$\text{(Angle of lap)} \quad \theta = 2 \operatorname{cosec}^{-1} \left(\frac{R-r}{S} \right) = 2.62 \text{ rad} \quad (4.1)$$

$$\text{(Speed ratio)} \quad \text{Speed ratio} = \frac{R}{r} = 2.6 \quad (4.2)$$

$$\text{(Velocity)} \quad v = \frac{\pi R N}{30} = 1.2246 \text{ ms}^{-1} \quad (4.3)$$

$$\text{(Belt area)} \quad A = \frac{m}{\rho} = 1.68 \times 10^{-4} \text{ m}^2 \quad (4.4)$$

$$\text{(Length of belt)} \quad L = r\theta + R(2\pi - \theta) + 2S \sin(\theta/2) = 1.21 \text{ m} \quad (4.5)$$

$$\text{(Tension on tight side)} \quad T_1 = (\text{max. stress})(\text{belt area}) = 1176.8 \text{ N} \quad (4.6)$$

$$\text{(Tension on slack side)} \quad T_2 = \frac{T_1}{e^{\mu\theta \operatorname{cosec} \beta}} = 469.4 \text{ N} \quad (4.7)$$

$$\text{(Power transmitted)} \quad P = V(T_1 - T_2) = 866.28 \text{ W} \quad (4.8)$$

$$\text{(Torque on the driver)} \quad \tau_1 = (T_1 - T_2)R = 91.96 \text{ Nm} \quad (4.9)$$

$$\text{(Torque on the follower)} \quad \tau_2 = (T_1 - T_2)r = 35.36 \text{ Nm} \quad (4.10)$$

By varying the smaller and larger pulley diameter and the center distance, we have identified the optimum conditions for our model to generate the maximum power.

Following the process, we have prepared an excel sheet on the whole optimum condition analysis containing the parameters like length of belt, angle of lap, speed ratios, tension on the tight and slack side, torque on the driver pulley and the follower, and the total power transmitted.

4.2.2 Varying smaller pulley diameter (d)

Firstly, we varied the diameter of the smaller pulley by small intervals and calculated the power, tensions and torque obtained. The maximum power acquired was (766.74 W) at (188 mm) diameter of the smaller pulley. The torque on the driver turned out to be (81.39 Nm) and on the follower it was (72.8 Nm). The tension on the tight side was (1175.93 N) and on the slack side we got (400.73 N). The center distance (S) and the larger pulley diameter was kept constant throughout i.e. (30 cm) and (210 mm).

Table 5 Varying smaller pulley diameter.

D	d	S	L	N_1	N_2	T_1	T_2	P	τ_d	τ_F
[mm]	[mm]	[cm]	[cm]	[rpm]	[rpm]	[N]	[N]	[W]	[Nm]	[Nm]
210	180	30	120.53	90	189	1164.46	400.56	755.57	80.20	68.75
210	184	30	121.12	90	189	1170.17	400.64	761.13	80.80	70.79
210	188	30	121.72	90	189	1175.93	400.73	766.74	81.39	72.86

4.2.3 Varying Larger pulley diameter (D)

Second, we varied the diameter of the larger pulley by small intervals and calculated the power, tensions and torque obtained. In this case, the maximum power generated was (874.3 W) at (266 mm) diameter of the larger pulley. The torque on the driver turned out to be (92.8 Nm) and on the follower it was (34.89 Nm). The tension on the tight side was (1171.46 N) and on the slack side we got (473.6 N). The center distance (S) and the smaller pulley diameter was kept constant throughout i.e. (30 cm) and (100 mm).

Table 6 Varying larger pulley diameter

D	d	S	L	N_1	N_2	T_1	T_2	P	τ_d	τ_F
[mm]	[mm]	[cm]	[cm]	[rpm]	[rpm]	[N]	[N]	[W]	[Nm]	[Nm]
250	100	30	117.78	90	225	1138.86	451.62	809.22	85.90	34.36

260	100	30	119.98	90	234	1159.13	465.25	849.71	90.20	34.69
266	100	30	121.26	90	239.4	1171.46	473.64	874.26	92.80	34.89

4.2.4 Varying center distance (S)

Last, we varied the center distance of the pulleys at the calculated optimum conditions of both smaller and larger pulley variations as elaborated above. On the larger pulley adjustment, we got the maximum power of (866.2 W) at a center distance of (30.1 cm). However, on the smaller pulley adjustment, we got the maximum power of (767.38 W) at a center distance of (30.05 cm). The smaller and the larger pulley diameters were kept constant throughout i.e. (100 mm) and (260 mm) on larger pulley adjustment and (188 mm) and (210 mm) on smaller pulley adjustment.

Table 7 Varying centre distance

D	d	S	L	N_1	N_2	T_1	T_2	P	τ_d	τ_F
[mm]	[mm]	[cm]	[cm]	[rpm]	[rpm]	[N]	[N]	[W]	[Nm]	[Nm]
260	100	28	116.35	90	234	1124.09	457.51	816.29	86.65	33.32
260	100	30	119.98	90	234	1159.13	465.25	849.71	90.20	34.69
260	100	31	121.81	90	234	1176.80	469.40	866.2	91.96	35.36

Table 8 Varying center distance of smaller pulley

D	d	S	L	N_1	N_2	T_1	T_2	P	τ_d	τ_F
[mm]	[mm]	[cm]	[cm]	[rpm]	[rpm]	[N]	[N]	[W]	[Nm]	[Nm]
210	188	29	119.75	90	189	1156.90	394.60	753.99	80.04	71.65
210	188	30	121.72	90	189	1175.93	400.73	766.74	81.39	72.86
210	188	30.05	121.82	90	189	1176.88	401.04	767.38	81.46	72.92

4.2.5 Final selection

After performing the analysis, we found the optimum condition for us which will be feasible for our model. These prime values of different parameters are listed below.

Table 9 Final selection

D	d	S	L	N₁	N₂	T₁	T₂	P	τ_d	τ_F
[mm]	[mm]	[cm]	[cm]	[rpm]	[rpm]	[N]	[N]	[W]	[Nm]	[Nm]
260	100	31	121.81	90	234	1176.80	469.40	866.2	91.96	35.36

4.2.6 Power Transmission using optimum conditions.

Following the process, we have plotted a bar chart indicating power transmitted using optimum condition of smaller pulley variation (PT_s), power transmitted using optimum condition of larger pulley variation (PT_l), power transmitted at a prime center distance using optimum condition of larger pulley (PT_{c2}), and power transmitted at a prime center distance using optimum condition of smaller pulley (PT_{c1}).

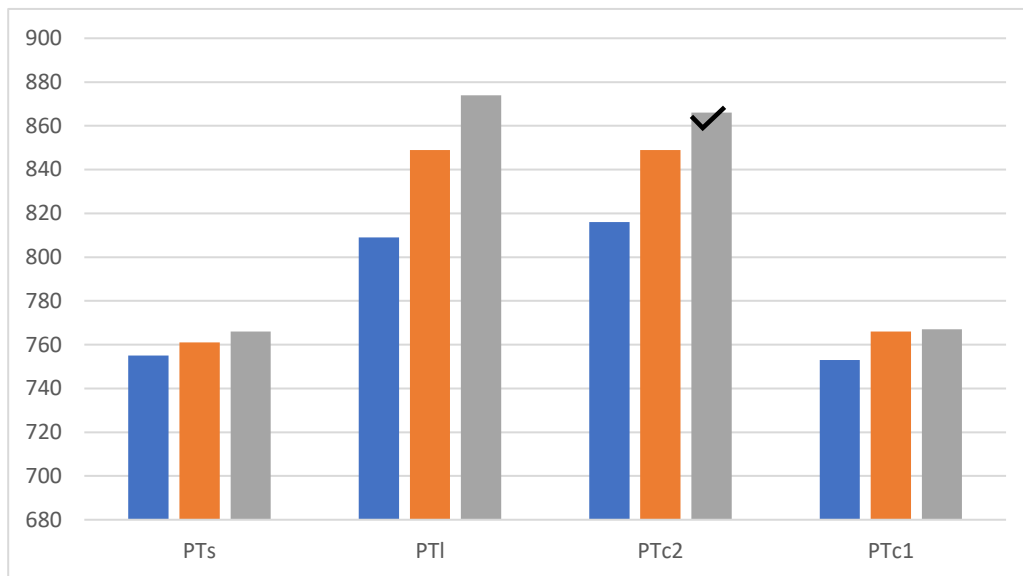


Figure 4.7 Power Transmitted trend

CHAPTER FIVE: POWER CALCULATIONS

After setting up our experiment, our next step was the power calculations. Firstly, we have calculated the point load of our pulleys which are putting their impact on the turbine causing the RPMs to decrease. Secondly, we have performed theoretical and experimental calculations on both the larger and smaller pulleys. Next, we have calculated the error produced. Following this, we selected our generator depending upon the rated RPMs and the power production through our system. Finally, we selected an LED bulb corresponding to our power production through generator.

$$\text{(Area of pulley)} \quad A = \pi r^2 = 0.212 \text{ m}^2 \quad (5.1)$$

$$\text{(Mass of pulley)} \quad m = 1.15 \text{ kg}$$

$$\text{(Point load)} \quad F = (w)(L) = 11.28 \text{ N} \quad (5.2)$$

5.1 Theoretical Calculations

5.1.1 Theoretical calculations on larger pulley

In the theoretical calculations of the larger pulley, we supposed the RPMs to be 90, dropping from 145 RPMs because of the weight domination of pulleys. Then, we calculated the torque and the angular velocity. Finally, we calculated the power which turned out to be 13.75 W.

$$\text{(Torque)} \quad T = (F)(r) = 1.46 \text{ Nm} \quad (5.3)$$

$$\text{(No of revolutions)} \quad N = 90 \text{ rpm (supposed)}$$

$$\text{(Angular velocity)} \quad \omega = \frac{2\pi N}{60} = 9.424 \text{ rad/s} \quad (5.4)$$

$$\text{(Power)} \quad P = (T)(\omega) = 13.759 \text{ W} \quad (5.5)$$

5.1.2 Theoretical calculations on smaller pulley

In the theoretical calculations of the smaller pulley, we knew that the pulley ratio was 1:3 i.e., 1 revolution of the larger pulley is equal to three revolutions of the smaller pulley. Therefore, multiplying 90 with 3, we got 270 RPMs on the smaller pulley. Then, we calculated the torque and the angular velocity. Finally, we calculated the power which turned out to be 1.38 W.

$$\text{(Torque)} \quad T = 4.9 \times 10^{-2} \text{ Nm} \quad \text{using eq. (5.3)}$$

$$\text{(No of revolutions)} \quad N = 270 \text{ rpm}$$

$$\text{(Angular velocity)} \quad \omega = 28.27 \text{ rad/s} \quad \text{using eq. (5.4)}$$

$$\text{(Power)} \quad P = 1.38 \text{ W} \quad \text{using eq. (5.5)}$$

5.2 Experimental Calculations

5.2.1 Experimental calculations on larger pulley

In the experimental calculations of the larger pulley, we recorded the RPMs to be 101 using tachometer on the larger pulley. In this case, we fixed the torque and by calculating the angular velocity we found the power which turned out to be 15.43 W.

(Torque) $T = 1.46 \text{ Nm}$ using eq. (5.3)

(No of revolutions) $N = 101 \text{ rpm}$

(Angular velocity) $\omega = 10.57 \text{ rad/s}$ using eq. (5.4)

(Power) $P = 15.43 \text{ W}$ using eq. (5.5)

5.2.2 Experimental calculations on smaller pulley

In the experimental calculations of the smaller pulley, we recorded the RPMs to be 303 using tachometer on the smaller pulley. In this case, we fixed the torque and by calculating the angular velocity we found the power which turned out to be 1.55 W.

(Torque) $T = 4.9 \times 10^{-2} \text{ Nm}$ using eq. (5.3)

(No of revolutions) $N = 303 \text{ rpm}$

(Angular velocity) $\omega = 31.71 \text{ rad/s}$ using eq. (5.4)

(Power) $P = 1.55 \text{ W}$ using eq. (5.5)

5.3 Error Calculations

5.3.1 Error on larger pulley

$$\text{Error} = \frac{15.43 - 13.759}{15.43} \times 100 = 10.8\%$$

5.3.2 Error on smaller pulley

$$\text{Error} = \frac{1.55 - 1.38}{1.55} \times 100 = 10.9\%$$

5.4 Generator Selection

To finally convert our mechanical energy into an electrical energy, we installed a DC generator of 12 volts having 2800 rated RPMs. This was the most suitable DC generator in

our case since our RPMs were low i.e., 303. More details of the specifications of the generator are listed below.

Nominal voltage	:	12 volts
Operating range	:	10.5 – 15 volts
No load current	:	0.56 A
Rated RPMs	:	2800

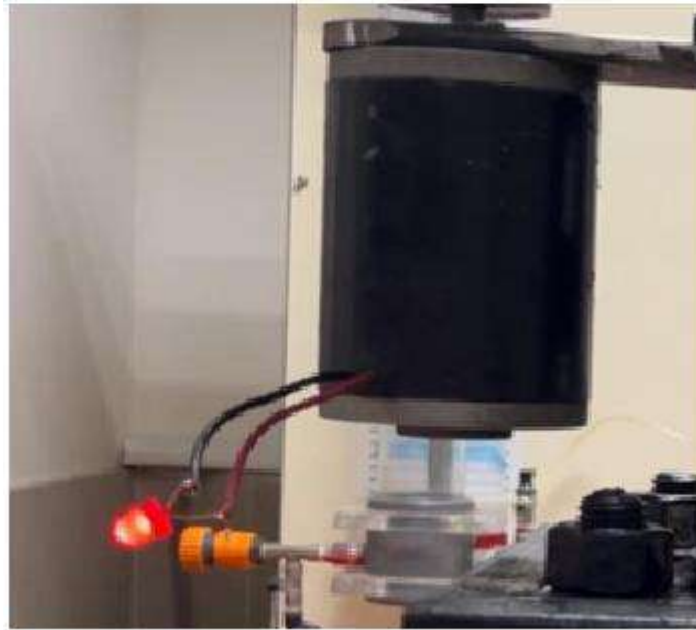


Figure 5.1 DC Generator

5.4.2 Generator power calculations

By installing a 12 volts DC generator having rated RPMs of 2800, we calculated our final power production through our system. Voltage range produced was 1.25 – 2 V. The current produced was 0.56 A having no load applied. By applying the load of pulleys, our current increased to 0.76 A. By using 1.25 V our power was 0.95 W, using 1.5 V our power was 1.14 W, and by using 2 V our power was 1.52 W. Thus, having low power production through our system, we installed a LED bulb having 1 Watt power and nominal voltage of 3 volts.

CHAPTER SIX: CONCLUSIONS AND FUTURE DIRECTION

In our opinion, this system can definitely generate more power and we can increase the overall efficiency as well. Following are the directions which can be adopted moving forward.

The inlet flowrate can be maintained and controlled more effectively using a reservoir mechanism at the inlet or by installing a gate at the neck of the runner. By doing so, we would be needing to control the overflow through the runner as well. Next up, the cone angle can be reduced and narrowed down by adding an acrylic sheet to decrease water seepage from the sides of the turbine and thus a complete analysis can be performed implanting this change. The shaft material can be switched to PVC or PLA material causing the weight to reduce and thus assisting us in generating more RPMs. Moreover, design of the blade can be switched to a bottom turned blade i.e., using same dimension of blades but turning it from the bottom side in order to provide more surface area of contact with water and thus have more RPMs achieved and then again performing the analysis and recording the data extracted. The number of blade wings can be increased or even decreased depending upon the designed geometry of the blades. The sections of our designed conical blade can be increased making sure that they are equally spaced all together. Also, an automated valve control system can be installed at outlet in order to maintain the inlet and outlet flowrates.

Our system was designed at a micro level having low flowrates and small basin area. The power production through our system is nearly maximum and all the conditions applied are optimum. In order to significantly increase our RPMs and ultimately our whole power production, we need to fabricate a larger system having larger basin area and higher flowrates. Thus, we will be able to design a relatively larger and more effective turbine depending upon the available conditions and ultimately generate more RPMs and power production.

Appendix 1

```
x=0:10;
y=[128 122 116 112 114 102 92 96 88 83 78];
plot(x,y, '--or');
hold on
ymax=[132 124 118 115 120 105 95 102 90 89 83];
plot(x,ymax);
hold on
ymin=[123 119.5 114 109 108 99 88 94 86 76 72];
plot(x,ymin);
hold on
y1=[103.5 102 90.5 92 83 84.5 71.5 74.5 67.5 64 52.5];
plot(x,y1, '--^');
hold on
y1max=[107 104 93 94 85 86 74 76 70 65 55];
plot(x,y1max);
hold on
y1min=[100 100 88 90 81 83 69 73 65 63 50];
plot(x,y1min);
hold on
y2=[87 82 75 71.5 69 62 55 40 30 21 14];
plot(x,y2, '--+');
hold on
y2max=[89 84 77 73 71 64 57 42 32 23 16];
plot(x,y2max);
hold on
y2min=[85 80 73 70 67 60 53 38 28 19 12];
plot(x,y2min);
hold off
xlabel('Blade Position -->');
ylabel('RPM -->');
title('RPM VS Blade Position');
```

Appendix 2

```
x=0:15;
y=[129 121.3 116.5 110 109 106.5 100.6 94.3 88 92 88.3 84 0 0 0 0];
plot(x,y,'--or');
hold on
y1=[111 114 110 105 99 102 97 92 84 88 81 0 0 0 0];
plot(x,y1,'--^');
hold on
y2=[145 131 126 121 128 118 119 109 123 112 108 99 75 83 71 74];
plot(x,y2,'--*');
hold off
xlabel('Blade Position');
ylabel('RPM');
title('RPM VS Blade Position');
```

Appendix 3

[13]

$$Q = \frac{2}{4.02} \times 0.001 = 0.00049 \text{ m}^3/\text{s}$$

$$Q = \frac{2}{3.89} \times 0.001 = 0.000514 \text{ m}^3/\text{s}$$

$$Q = \frac{2}{2.32} \times 0.001 = 0.00086 \text{ m}^3/\text{s}$$

$$Q_{av} = 0.000236 \text{ m}^3/\text{s}$$

$$Q_{av} = 0.00193 \text{ m}^3/\text{s}$$

$$D = 1.5(0.0254) = 0.0381\text{m}$$

$$V_{avg} = 1.67 \text{ m/s}$$

$$3 \text{ meshed Conical Blade (HR)} = \frac{16.2}{25} = 0.64$$

$$2 \text{ (upper) meshed Conical Blade (HR)} = \frac{12.7}{25} = 0.51$$

$$2 \text{ (lower) meshed Conical Blade (HR)} = \frac{7}{25} = 0.28$$

$$\text{Speed Ratio} = \frac{R}{r} = \frac{13}{5} = 2.6$$

$$V = \frac{\pi R N}{30} = \pi \frac{13 \times 10^{-2} \times 90}{30} = 1.2246 \text{ ms}^{-1}$$

$$A = \frac{m}{\rho} = \frac{0.2037}{1200} = 1.68 \times 10^{-4} \text{ m}^2$$

$$L = r\theta + R(2\pi - \theta) + 2S \sin(\theta/2)$$

$$L = 121.8 \text{ cm} = 1.21 \text{ m}$$

$$T_1 = \text{max. stress} \cdot \text{belt area} = 7 \times 10^6 \times 1.68 \times 10^{-4} = 1176.8 \text{ N}$$

$$T_2 = \frac{T_1}{e^{\mu \theta \operatorname{cosec} \beta}} = \frac{1176.8}{e^{0.12 \times 2.62 \times 2.9}} = 469.4 \text{ N}$$

$$P = V(T_1 - T_2) = 0.98 (1176.8 - 469.4) = 866.28 \text{ W}$$

$$\tau_1 = (T_1 - T_2)R = 91.96 \text{ Nm}$$

$$\tau_2 = (T_1 - T_2)r = 35.36 \text{ Nm}$$

$$A = \pi(0.260)^2 = 0.212 \text{ m}^2$$

$$m = 1.15 \text{ kg}$$

$$F = w = mg = 1.15 \times 9.81 = 11.28 \text{ N}$$

$$w = \frac{F}{L} = \frac{11.28}{0.26} = 43.38 \frac{\text{N}}{\text{m}}$$

$$\text{Point Load} = w \times L = 43.38 \times 0.26 = 11.28 \text{ N}$$

$$T = F \cdot R = 11.28 \times 0.13 = 1.46 \text{ Nm}$$

$$N = 90 \text{ rpm (supposed)}$$

$$\omega = \frac{2\pi N}{60} = \frac{2\pi(90)}{60} = 9.424 \text{ rad/s}$$

$$P = T \cdot \omega = 1.46 \times 9.424 = 13.759 \text{ W}$$

$$T = F \cdot r = 0.981 \times 0.05 = 0.0490 \text{ Nm}$$

$$N = 90 \times 3 = 270$$

$$\omega = \frac{2\pi N}{60} = \frac{2\pi(270)}{60} = 28.27 \text{ rad/s}$$

$$P = T \cdot \omega = 0.0490 \times 28.27 = 1.38 \text{ W}$$

$$T = 11.28 \times 0.13 = 1.46 \text{ Nm}$$

$$N = 101 \text{ Rpm}$$

$$\omega = \frac{2\pi N}{60} = \frac{2\pi(101)}{60} = 10.57 \text{ rad/s}$$

$$P = T \cdot \omega = 1.46 \times 10.57 = 15.43 \text{ W}$$

$$T = 0.981 \times 0.05 = 0.0490 \text{ Nm}$$

$$\omega = \frac{2\pi N}{60} = \frac{2\pi(303)}{60} = 31.71 \text{ rad/s}$$

$$P = T \cdot \omega = 0.0490 \times 31.71 = 1.55 \text{ W}$$

$$P = VI = 1.25 \times 0.76 = 0.95 \text{ W}$$

$$P = VI = 1.5 \times 0.76 = 1.14 \text{ W}$$

$$P = VI = 2 \times 0.76 = 1.52 \text{ W}$$

References

- [1] Travieso-Rodriguez, J. A., Jerez-Mesa, R., Llumà, J., Traver-Ramos, O., Gomez-Gras, G., & Roa Rovira, J. J. (2019). Mechanical Properties of 3D-Printing Polylactic Acid Parts subjected to Bending Stress and Fatigue Testing. *Materials*, 12(23), 3859. <https://doi.org/10.3390/ma12233859>
- [2] Abdul Aziz, M. Q. ., Juferi Idris, & Muhammad Firdaus Abdullah. (2022). Simulation of the Conical Gravitational Water Vortex Turbine (GWVT) Design in Producing Optimum Force for Energy Production. *Journal of Advanced Research in Fluid Mechanics and Thermal Sciences*, 89(2), 99–113. <https://doi.org/10.37934/arfmts.89.2.99113>
- [3] Tri Ratna Bajracharya, Shree Raj Shakya, Ashesh Babu Timilsina, Jhalak Dhakal, Subash Neupane, Ankit Gautam, Anil Sapkota, "Effects of Geometrical Parameters in Gravitational Water Vortex Turbines with Conical Basin", *Journal of Renewable Energy*, vol. 2020, Article ID 5373784, 16 pages, 2020. <https://doi.org/10.1155/2020/5373784>
- [4] Wanchat, S., Suntivarakorn, R., Wanchat, S., Tonmit, K., & Kayanyiem, P. (2013). A Parametric Study of a Gravitation Vortex Power Plant. *Advanced Materials Research*, 805–806, 811–817. <https://doi.org/10.4028/www.scientific.net/amr.805-806.811>
- [5] DOMESTIC MICRO HYDRO POWER PLANT. (2015)
- [6] Pritchard-Fox-McDonalds_2011_8ed_Fluid-Mechanics. (n.d.).
- [7] Turbulent Plant in Indonesia. (n.d.).
- [8] Uta pressbook. (n.d.).
- [9] Theory of Machines / Belt Drives
- [10] Mockmore, C. A. (1949). The Banki Water Turbine Engineering Experiment Station Oregon State System of Higher Education Oregon State College Corvallis.

- [11] Dhakal, S., Timilsina, A. B., Dhakal, R., Fuyal, D., Bajracharya, T. R., Pandit, H. P., Amatya, N., & Nakarmi, A. M. (2015). Comparison of cylindrical and conical basins with optimum position of runner: Gravitational water vortex power plant. In *Renewable and Sustainable Energy Reviews* (Vol. 48, pp. 662–669). Elsevier Ltd. <https://doi.org/10.1016/j.rser.2015.04.030>
- [12] e e publishers, April 23rd, 2018. *The gravitational vortex water turbine puts small hydro on the map*[online] Available at <http://www.ee.co.za/article/the-gravitational-vortex-water-turbine-puts-a-spin-on-small-hydro.html>
- [13] Theory of machines by S S Rattan

